Canada

AD-A172 045

AN EXPERIMENTAL INVESTIGATION OF SKIN FRICTION ON SMOOTH SURFACES SUPPORTING AIR BEARING CHANNELS

by

M. Khalid
National Aeronautical Establishment

DTIC FILE COPY

National Research   Conseil national
Council Canada   de recherches Canada

86   8 15 174

NATIONAL AERONAUTICAL ESTABLISHMENT

SCIENTIFIC AND TECHNICAL PUBLICATIONS

AERONAUTICAL REPORTS:

Aeronautical Reports (LR): Scientific and technical information pertaining to aeronautics considered important, complete, and a lasting contribution to existing knowledge.

Mechanical Engineering Reports (MS): Scientific and technical information pertaining to investigations outside aeronautics considered important, complete, and a lasting contribution to existing knowledge.

AERONAUTICAL NOTES (AN): Information less broad in scope but nevertheless of importance as a contribution to existing knowledge.

LABORATORY TECHNICAL REPORTS (LTR): Information receiving limited distribution because of preliminary data, security classification, proprietary, or other reasons.

Details on the availability of these publications may be obtained from:

> Publications Section,
> National Research Council Canada,
> National Aeronautical Establishment,
> Bldg. M-16, Room 204,
> Montreal Road,
> Ottawa, Ontario
> K1A 0R6

ÉTABLISSEMENT AÉRONAUTIQUE NATIONAL

PUBLICATIONS SCIENTIFIQUES ET TECHNIQUES

RAPPORTS D'AÉRONAUTIQUE

Rapports d'aéronautique (LR): Informations scientifiques et techniques touchant l'aéronautique jugées importantes, complètes et durables en termes de contribution aux connaissances actuelles.

Rapports de génie mécanique (MS): Informations scientifiques et techniques sur la recherche externe à l'aéronautique jugées importantes, complètes et durables en termes de contribution aux connaissances actuelles.

CAHIERS D'AÉRONAUTIQUE (AN): Informations de moindre portée mais importantes en termes d'accroissement des connaissances.

RAPPORTS TECHNIQUES DE LABORATOIRE (LTR): Informations peu disséminées pour des raisons d'usage secret, de droit de propriété ou autres ou parce qu'elles constituent des données préliminaires.

Les publications ci-dessus peuvent être obtenues à l'adresse suivante:

> Section des publications
> Conseil national de recherches Canada
> Établissement aéronautique national
> Im. M-16, pièce 204
> Chemin de Montréal
> Ottawa (Ontario)
> K1A 0R6

AN EXPERIMENTAL INVESTIGATION OF SKIN FRICTION ON SMOOTH SURFACES SUPPORTING AIR BEARING CHANNELS

ÉTUDE EXPÉRIMENTALE DU FROTTEMENT PELLICULAIRE SUR DES SURFACES LISSES PORTEUSES DE CANAUX ANTI-FROTTEMENT

by/par

M. Khalid

National Aeronautical Establishment

L.H. Ohman, Head/Chef
High Speed Aerodynamics Laboratory/
Laboratoire d'aérodynamique à hautes vitesses

W. Wallace
Acting Director/
Directeur Intérimaire

SUMMARY

A new method, to obtain skin friction reduction by installing air-bearing channels on a smooth surface in uniform flow was investigated. The measurements were made by a servo-controlled skin friction balance. The parametric studies of the channel having step dimensions less than the laminar sublayer thicknesses and placed in flows of free stream velocity up to 90 ft/s have shown that an average skin friction reduction of 25% in the air-bearing cavity is well within reach. It was also confirmed that riblet-type surface grooves can produce up to 10% skin friction drag reduction.

RÉSUMÉ

On étudie une nouvelle méthode pour réduire le frottment pelliculaire sur une surface lisse exposée à un écoulement uniforme en installant sur la surface des canaux qui agissent comme des paliers d'air. Les mesures ont été prises à l'aide d'une balance de mesure du frottement pelliculaire servocommandée. Les études paramétriques des cannaux dont les dimensions de la section sont inférieures aux épaisseurs des sous-couches laminaires et qui ont été exposés à des écoulements libres allant jusqu'à 90 m/s montrent qu'il est fort possible de réduire le frottement pelliculaire de 25% en moyenne dans les cavités anti-frottement. Il a aussi été confirmé que des rainures dont les bords émergent de la surface peuvent réduire la traînée due au frottement pelliculaire dans une proportion allant jusqu'à 10%.

CONTENTS

ILLUSTRATIONS

ILLUSTRATIONS (Cont'd)

1.0 INTRODUCTION

In the past decade or so, the aerodynamic community at large has made a serious effort to find new ways of reducing fuel consumption for all types of vehicles.

The concern for more efficient air transport system has promoted research into the design of lower drag airfoil shapes (Ref. 1) including a renewal of interest in boundary layer control mechanisms. From the latter a number of ingenious devices have evolved including LEBU's (large eddy break up units), riblets, air bubbles and micro air-bearings. Other ideas involve means of providing compliant surfaces for control of boundary layer profiles, contamination of the flow with viscosity lowering substances and Emmons Spot Modification. References (2), (3) and (4) describe work on the various means.

The National Aeronautical Establishment, through High Speed Aerodynamics Laboratory has also been active in exploring drag reduction ideas. From early in the last decade NAE has worked quite closely with DeHavilland Aircraft Company of Canada on the augmentor wing concept (a means of improving aerodynamic efficiency in STOL and in cruise flight) and in the development of airfoil sections. Whittley (5) has given an up to date account of the progress made on the augmentor wing and references to the augmentor wing experiments conducted in the HSAL's high Reynolds number, 2D and 5 ft facilities are contained in the report, Ref. (6).

In airfoil section development, more recently, NAE has been very active in a joint NRC PILP project with DeHavilland Canada to investigate a series of supercritical airfoils $(0.1 < t/c < 0.21)$.

These by virtue of supporting large regions of natural laminar flow lead to substantial drag reductions. The results obtained from this study so far, have been reported in Refs. (7) and (8).

NAE also had some involvement with Canadair Ltd of Canada in a study of energy efficiency supercritical wings (9).

The present study was carried out with the broad objective of investigating some of the novel techniques (e.g. LEBU's, riblets etc.) currently described in the literature (10) as means of drag reduction. It was during this investigation that it was noticed quite accidentaly that finite size channel air-bearings can lead to a substantial skin friction drag reduction.

This note reports some of the drag measurements obtained in the present study. Most data was obtained by use of a recently acquired half-inch diameter skin friction balance in a 5" × 5" low speed research facility. The first part of the note deals with the comparison of the skin friction data measured on a smooth plate using the balance, against theoretical predictions. The second part reports on the riblet studies and the confirmation that suitably scaled riblets can lead to as much as 10% reduction in skin drag. The last part investigates the channel air-bearing concept (rectangular cavities formed by suitably scaled edges).

2.0 THE FACILITY

The 5" × 5" low speed research facility of HSAL was used for most of the present experimental work. It was converted to its current square cross section tunnel format from the original open jet mode by

installing a new contraction and nozzle, followed by a working section and a downstream diffuser. See Ref. (11) for the features which are common to both modes (Filter Box, Air Supply, Settling Chamber and Upstream Diffuser). The remaining parts of the facility are described with the aid of the photograph in Fig. (1a), and the diagram in Fig. (1b).

The air is supplied from a blower having a maximum of 4200 rev/min. The blower is driven by a 5 h.p. constant speed motor such that flow pulsation can be minimized. The speed of the blower can be varied from 3560 to 4200 r.p.m. through a set of adjustable pitch up pullies.

The 3 ft long contraction section is made of formed fibreglass with an inlet diameter of 24" and an outlet of 9" square cross section. The profiled nozzle is also made of formed fibreglass and bolts on to the contraction with a 16 mesh steel screen placed in between. The nozzle has an exit cross section of 5" sq. The effective contraction ratio of the profiled nozzle is about 0.66.

The nozzle is connected to a 4 ft long working section having a 5" sq cross section. The removable walls of the working section which provide access from all four sides are made from smooth plexi-glass materials. The working section in turn joins onto a diffuser which exhausts the flow to the atmosphere about 30" downstream of the working section. The outlet of the diffuser is a 9" sq cross section. A photograph of the working section area of this facility is given in Fig. (1).

A calibration curve of the flow velocity derived from the measured pressure difference between the centre line pitot pressure and the wall static pressure versus settling chamber stagnation pressure is plotted in Fig. (2). The measurement station for the pitot-static pressure data was 30" downstream of the entrance of the test section.

3.0 SKIN FRICTION BALANCE

A servo-controlled balance developed by the Laval University, Quebec was used for direct skin friction measurements. Reference (12) provides an adequate description of the balance and the principle on which it operates. Two photographs of the balance are given in Fig. (3a) and (3b).

The balance was calibrated according to the procedure recommended in Ref. (12) and it was found to have a calibration factor of 1 mv/mg. The skin friction drag is sensed by a floating element which is 0.495 in. in diameter and lies flush with the remaining surface of the balance. The balance itself is accommodated in a suitably designed cavity in the tunnel wall such that the top surface of the balance housing the above floating element lies flush with the wall surface.

As a precautionary measure, when used in the NAE blowdown facilities, the top surface of the balance housing is drilled with a number of holes in order to minimize the effect of pressure differences between the top surface and the cavity which houses the balance mechanisms due to starting and stopping transients (Fig. 1b). The

balance sensing element can mainly be damaged by too large a pressure difference.

The skin friction coefficient C_f is obtained by the relationship:

$$C_f = \frac{F_w}{\frac{1}{2}\rho U_\infty^2 S_E} = \frac{\tau_w}{\frac{1}{2}\rho U_\infty^2} \qquad (1)$$

where;

F_w is the force measured by the sensing element,

S_E is the surface area of the sensing element,

ρ is the air density,

U_∞ is the free stream velocity.

τ_w is F_w/S_E

4.0 SKIN FRICTION MEASUREMENTS

4.1 On a Smooth Plate

The cavity see Fig. (1b), which houses the skin friction balance is situated in the working section area about 30" downstream of the nozzle. The boundary layer flow at this station is turbulent, with the Reynolds Number being in the range, $0.253 \times 10^6 < Re/ft < 0.583 \times 10^6$.

At a number of tunnel conditions ranging from $U_\infty = 39.7$ ft/s to 91.5 ft/s, skin friction measurements on a smooth surface were recorded using the balance.

In addition to the balance measurements, boundary layer velocity profiles were obtained at the same position as the balance sensing head using a 0.095" diameter traversing pitot-probe from which

data the local skin friction can be derived. The probe displacement
effect following Ref (13) was found to be negligible.

The local skin friction can be calculated from the velocity
profile data according to the relationship, from Ref (14).

$$C_f = 0.246 \times 10^{-0.678H} \left(\frac{U_\infty \theta}{\nu}\right)^{-0.268} \tag{2}$$

where the Form parameter $H = \theta/\delta^*$

Momentum thickness $\qquad \theta = \int_0^\infty \frac{U}{U_\infty} \left(1 - \frac{U}{U_\infty}\right) dy$

Displacement thickness $\qquad \delta^* = \int_0^\infty \left(1 - \frac{U}{U_\infty}\right) dy$

U = local velocity

ν = kinematic viscosity

y = distance from the surface

A Clauser plot of these velocity profiles is presented as $\frac{U}{U_\tau}$
versus $\text{Log}\left(\frac{yU_\tau}{\nu}\right)$ graph in Fig. (4), where the friction velocity
$U_\tau = \sqrt{\tau_w/\rho}$ for each velocity profile was separately evaluated from the
skin friction measurement. The convergence of the data at six
different flow conditions demonstrates the similitude in velocity
profile shapes.

Figure (5) shows the comparison of skin friction values as
obtained from the above two methods when plotted against Reynolds
number based on momentum thickness, $Re(\theta) = \frac{U_\infty \theta}{\nu}$. Except for the last
point which shows a discrepancy of about 4% in the two methods, the
agreement is very good.

Figure (6) shows a similar plot of C_f against the local Reynolds number, $Re(x) = U_\infty x/\nu$. Also shown on this graph is the theoretical relationship of C_f vs $Re(x)$ based on the equation,

$$C_f(x) = 0.455\ln^{-2}(0.06\ Re(x)) . \qquad (3)$$

NOTE: x - is the distance between the virtual origin of the boundary layer starting point to the station where the balance sensing element is located. Equation (3) as described in Ref. (15), is derived from Spalding's Law of Wall formula and is claimed to be accurate to $\pm2\%$, for the entire turbulent range. The agreement amongst the data is quite satisfactory.

It may be of interest to mention that the skin friction measurements were also made at higher Reynolds number range $10^6 \leq Re(x) \leq 16 \times 10^6$ in the NAE 5" $\times$ 5" blowdown pilot facility. See Ref. (16) for a description of the pilot facility. Figure (7) shows the comparison between the balance measurements of the skin friction and theoretical prediction based on Eq. (3). The balance data compares quite well with the theoretical predictions.

4.2 Riblet, Skin Friction Measurements

In recent years riblets have received a great deal of attention from the aerodynamic community as an effective means of reducing skin friction drag. It is argued that the grooved shapes have a damping effect upon the turbulent bursting process consequently reducing the aerodynamic drag. References (10), (17) and (18) amongst others have reported skin friction measurements using this particular

technique. In some cases a drag reduction of up to 10% has been claimed, Ref. (17).

Figure (8) provided by the 3M Center, Minnessota depicts some of the riblet geometries and associated dimensions which have been used in the above references. The riblet material used in this study was also obtained from the same source.

Walsh and Lindemann, Ref. (17), have suggested the scaling of the amplitude h and the pitch s of the riblet grooves to follow the relationships:

$$h^+ = \frac{hU_\infty}{\nu} \sqrt{\frac{C_{f_o}}{2}} \qquad (4)$$

$$s^+ = \frac{sU_\infty}{\nu} \sqrt{\frac{C_{f_o}}{2}} \qquad (5)$$

where

C_{f_o} - skin friction coefficient corresponding to smooth flat plate value.

It was further established from the results available in Ref. (17) that $h^+ \simeq s^+ \simeq 15$ were the best values of the scaling parameters on which to base the dimensions of the riblet. It was, therefore, decided to use the riblets DA-3015B, DA-3015C and DA-3015E [see Fig. (8)] in the present experiments, as these models came closest to satisfying the scaling requirements.

When measuring the local skin friction as sensed by the balance element, it was found that the riblet material could not be successfully installed on top of the element. This difficulty arose

from the fragility of the mechanism which supports the element. Any normal force during installation or detachment will almost certainly damage the mechanism.

As an alternative, the local skin friction C_f was measured at predetermined distances downstream of the riblet sheet. This approach, does not give the exact effect of the riblets upon C_f locally, but, any difference detected in drag where the sensing element is stationed does provide an indication of the lasting effect of the riblets.

Some interesting results obtained from the riblet experiments are as follows:

Figure (9) shows the skin friction values at a range of freestream flow conditions for the three riblet sheets DA-3015B, DA-3015C and DA-3015E normalized with respect to the "smooth sheet" value C_{f_s} (having the same thickness as the riblet sheets) and plotted against the scaling parameter s^+. Note that the smooth sheet value was obtained by replacing the riblet sheet with a smooth sheet of the same thickness as the maximum thickness of riblet sheets. The distance between the trailing edge of riblet sheet (or the smooth sheet) and the sensing element was 1.2". It is noted that in the range $s^+ < 20$, DA-3015E gives the best drag reduction of 7.5%. Beyond this range $s^+ > 20$, DA-3015C appears to be most effective providing a drag reduction of 4.5% at $s^+ = 30$. It should be understood that the basic h and s dimensions of riblets DA-3015C and DA-3015B prevent them from occupying any s^+ value in the range $s^+ < 20$.

Figure (10) shows a comparison of skin friction measurements for different riblet sheets and the corresponding smooth sheet at

uniform flow velocities of 39.0, 65.2 and 91.5 ft/s. The experimental arrangement is called configuration (1).

The skin friction as plotted in Figure (10) has been normalized with respect to the smooth surface value C_{f_o} (with no obstruction grooved or smooth between upstream flow and the sensing element). Within the error margin of the experiment there is very little to choose between the riblets and the corresponding smooth sheet. The graphs do however indicate a certain trend in skin friction values as the sensing element is moved away from the sheet. It is noted that the local skin friction is at its lowest value when the sensing element is closest to it. As the sensing element is moved downstream the skin friction rises quickly (In some cases above the smooth surface value C_{f_o}) and approaches the smooth surface value as x becomes large, $x > 0.9$ in.. This behaviour of the skin friction was studied in more detail in some of the latter experiments.

The scaling procedures mentioned earlier show that for high Reynolds number regimes $Re/ft > 10^6$ the size of the riblets (amplitude and pitch) becomes so small that their manufacture and availability is difficult. For example, at a Reynolds number of $Re/ft = 10^6$, the h and s dimension of a riblet would have to be about 3.7×10^{-3} in order to satisfy the optimum h^+ and s^+ scaling values of 15. These h and s dimensions would drop still further by nearly an order of magnitude if the Reynolds number, Re/f+ is increased to 10×10^6.

4.3 The Air-Bearing Channel Experiment

It is fairly well known (see Ref. (19)) that if the size of a protuberance in a given flow remains within a certain height dimension

then the basic characteristics of the boundary layer remain unaltered.
Rotta (14) suggests that the maximum size of the obstacle is governed
by the laminar sublayer thickness which is approximately defined by the
relationship.

$$\frac{U_\tau \delta_s}{\nu} \cong 60$$

δ_s - sublayer thickness

U_τ can be easily evaluated by measuring the wall shear stress τ_w using
the skin friction balance and computing U_τ from the definition
$U_\tau = \sqrt{\tau_w/\rho}$. In the 5"×5" low speed tunnel, the value of the sublayer
thickness was found to be about $\delta_s = 0.029$ inches, at a free stream
velocity of $U_\infty = 90$ ft/s.

The air-bearing channel experiment was basically designed to
study the skin friction behaviour in the lateral rectangular cavity
bounded by strips with a thickness less than the thickness of the
boundary layer sublayer. This particular geometry of the air-bearing
channel having finite gap width and a step dimension of the order of
the sublayer thickness makes it different from the micro air-bearings
(10) or the gaps formed by large roughness (20). The parameters
investigated in this exercise included the effect of the width of the
gap between the strips, the width and the thickness of the strips, and
the distance from the balance sensing element from the upstream (and/or
downstream) strip edge. The strip material was the same as the riblet
sheets used earlier or alternatively a plain smooth surfaced adhesive
tape.

Figure (11) shows the skin friction variation along the gaps whose width ranged within the limits $0.5" \leq \Delta \leq 2.5"$. This arrangement of strips is called configuration (2). The minimum permissible gap width $\Delta = 0.5"$ is understandably equal to the diameter of the sensing element of the skin friction balance. The skin friction seems to increase sharply from a low of about 55% of the smooth surface value C_{f_o} as the sensing element is moved downstream, and approaches a maximum of about 110% of the smooth surface value at x about $0.4 - 0.5"$. The skin friction then gradually reduces back to about 60% of the smooth surface value as the sensing element approached the aft-strip. This behaviour was found to be true for most gap-studies with the trends being more pronounced in some cases. The minimum gap value of $\Delta = 0.5"$, gave the best constant C_f/C_{f_o} value of about 0.36.

Two, 1.5" wide sheets from riblet DA-3015C were used to form the channel in which above skin friction traverses were made. The overall thickness of the riblet sheet was about 0.023".

Figure (12) demonstrates the effect of the strip thickness, τ_{thick}, upon skin friction measured in two gap sizes. It is clear that skin friction reduces in the air-bearing channel as the τ_{thick} increases. Once again the minimum 0.5" gap gives the best performance, with the skin friction in the air-bearing channel always remaining below the smooth surface value, C_{f_o}. For the 0.75" gap, the skin friction was measured against τ_{thick} for three different positions of the sensing element. The lowest value of skin friction was always detected when the element was closest to the upstream strip.

The results plotted in Fig. (13) show that the skin friction is almost invariant with strip width. It should be noted, however, that these results were obtained for a fixed gap of 0.5". The riblet-sensing element arrangement here was called configuration (2).

Figure (14) shows the skin friction immediately in front of a strip, studied under an arrangement called configuration (3). Three types of strips were used in this experiment. All indicate a gradual build up in drag from a minimum of around 50% of the smooth surface value C_{f_o} when the sensing element is immediately next to the strip; to a maximum approaching the smooth surface value as the sensing element moves upstream away from the strip.

A similar experiment to study the downstream effect of the individual strip upon skin friction was also carried out. This strip arrangement is called configuration (4). The results are shown in Fig. (15). The same three strips from configuration (3) were again used in this experiment. The plots indicate a sharp rise in skin friction from a low value (about 60% for two strips with τ_{thick}= 0.023 and 23% for τ_{thick} = 0.032) when the sensing element and strip are side by side to a high value (about 120%) as the element moves away from the strip. Again the grooved riblet and the smooth surface strip, both with τ_{thick}= 0.023, give similar performance.

The above reported results have shown some significant reductions in skin friction in an air-bearing channel. The gap widths studied under configuration (2) Fig. (11) give an average reduction of 25% in skin friction. With the thickness of the strips less than the

thickness of the laminar sublayer the strip edges in theory do not produce any protuberance drag. However, this has to be verified by measuring the total drag of a flat plate supporting a number of these air-bearing channels. Design is under way at NAE for such a 'flat plate' balance. It may be allowed to speculate that by using riblet material to form the air-bearing channels we can capitalize on both techniques and achieve a significant overall reduction in skin friction.

5.0 CONCLUSION

The servo-controlled skin friction balance designed by Laval University of Quebec has proved to be a very convenient and accurate tool for direct measurements of local skin friction on aerodynamic surfaces.

Measurements obtained from the skin friction balance on a smooth plate are in good agreement with the corresponding values derived from the velocity-traverses in the boundary layer.

The axial measurements of local skin friction $C_f(x)$ were also in good agreement with the predictions from the flat plate skin friction relationship, $C_f(x) = 0.455 \ln^{-2}(0.06\ \text{Re}(x))$.

At low Reynolds numbers, with proper scaling the riblets can be used quite effectively to reduce skin friction drag by as much as 10%.

A new method of reducing skin friction by installing air-bearing channels on aerodynamic surfaces has been investigated. Skin friction drag reduction of almost 70 - 80% has been measured

inside a channel of width 0.5" and a depth of .023", i.e. within the

thickness of the laminar sublayer.

Further experiments are required to measure the <u>total drag</u> on

a smooth plate supporting the riblet channel air-bearings.

9. Whyte, P.H. 'High Speed Wind Tunnel Test Program at the NRC 5 ft ×
    5 ft blowdown wind tunnel as part of the energy efficient aircraft
    study', Canadair-AD-80-17, September 1980.

10. Bushnell, D.M., Anders, J.B., Walsh, M.J. and McInville, R.V.
    'Turbulent drag reduction research', AGARD, CP-365, Brussels,
    May 21-23, 1984.

11. Lee, B.H.K., and Payne, L.F., 'Turbulence and Wave Measurements in
    a subsonic jet', LTR-HA-32, June 1974.

12. Nguyen, V.D., Dickinson, J., et al. 'Some experimental
    observations of the law of the wall behind large eddy breakup
    devices using servo controlled skin friction balances',
    AIAA-84-0346, January 9-12, 1984.

13. Livesey, J.L. 'The behavior of transverse cylindrical and forward
    facing total pressure probes in transverse total pressure
    gradient', Journal of Aeronautical Sciences, Oct. 1956.

14. Rotta, J.C. 'Boundary Layer Problems', published in Progress in
    Aeroauntical Sciences Series, Vol. 2, pp. 153-219 Pergamon Press
    1962.

15. White, F.M., 'Viscous Fluid Flow', pp. 497-498 McGraw-Hill
    Publishers 1974.

16. Elfstrom, G.M., Lockyear, S.J., and Lanovette, J.G., 'Tests on
    temperature recovery probes in the NAE 5" × 5" test facility',
    LTR-HA-5×5/0116, October 1977.

17. Walsh, M.J. and Lindemann, A.M. 'Optimization and application of
    riblets for turbulent drag reduction', presented at the AIAA 22nd
    Aerospace Sciences Meeting, Reno, Nevada, January 9-12, 1984.

18. Bushnell, D.M. 'Turbulent drag reduction for external flows', Aircraft Drag Prediction and Reduction AGARD Report No. 723 from NASA, VKI Turbulence course.

19. Schlichting, H. 'Boundary Layer Theory', 7th edition, McGraw-Hill series in Mechanical Engineering, 1979.

20. Liu, C.K., Kline, S.J., and Johnston, J.P., 'An experimental study of turbulent boundary layers on rough walls', Report MD-15 Stanford University, California, July 1966.
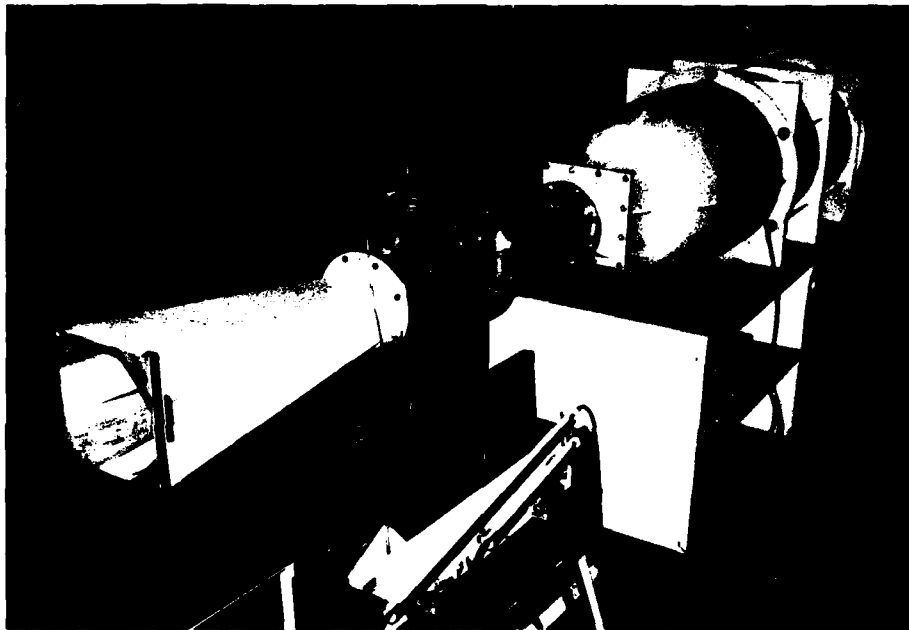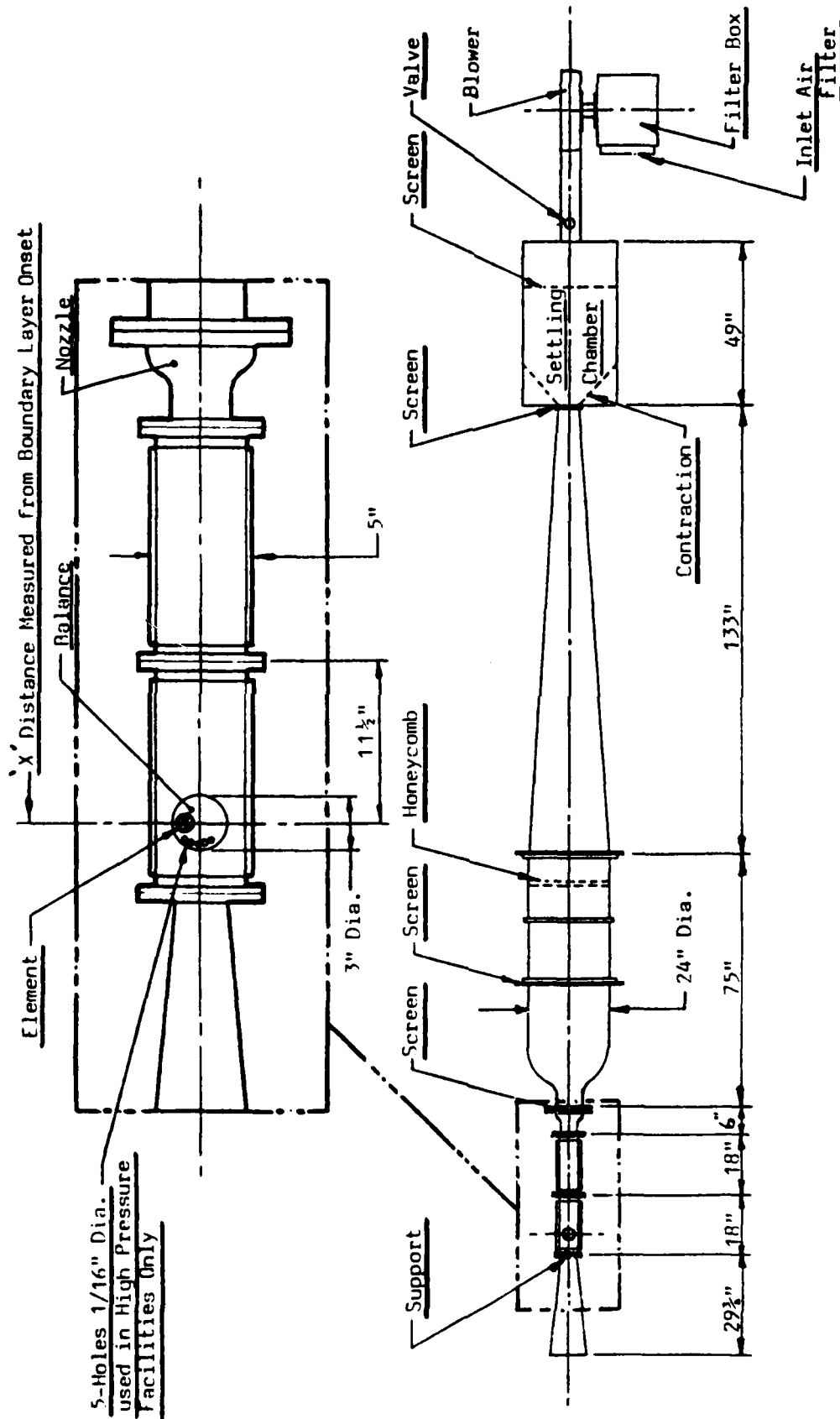
FIG. 1a: NAE 5-IN. X 5-IN. LOW SPEED RESEARCH FACILITY

FIG. 1b: SCHEMATIC OF LOW SPEED FACILITY
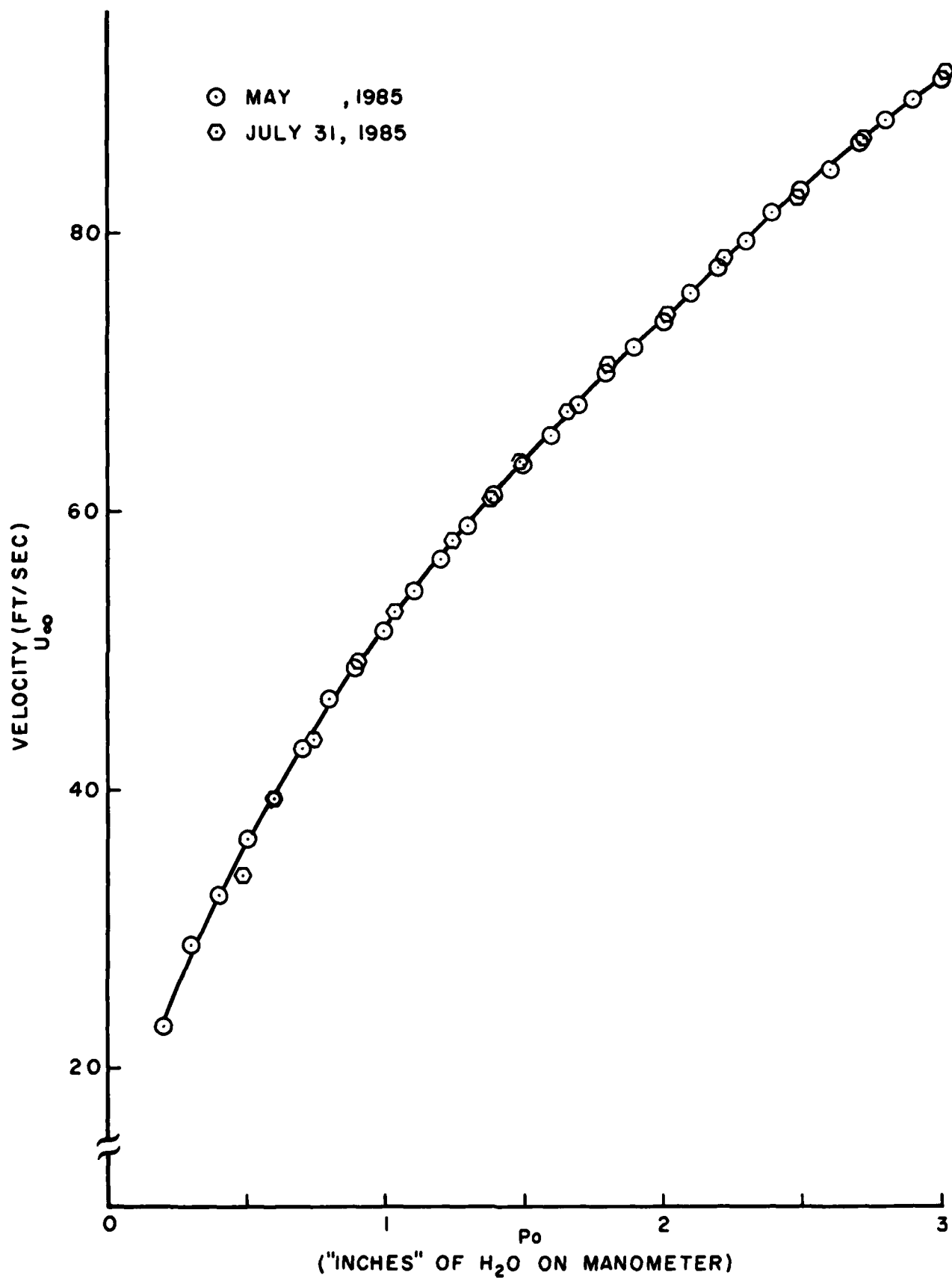
FIG. 2: CALIBRATION CURVE

FIG. 3a: SKIN FRICTION BALANCE
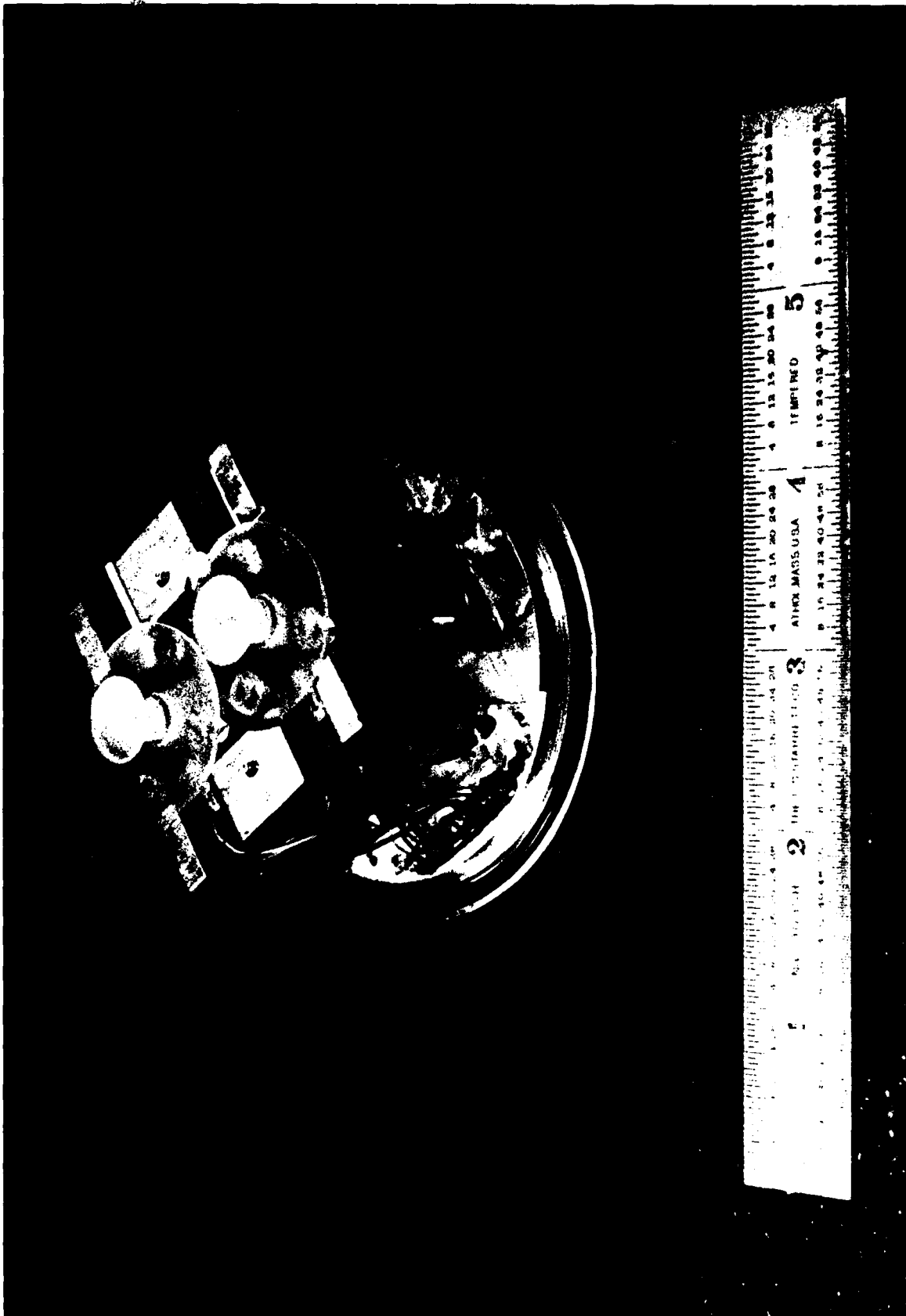
FIG. 3b: SKIN FRICTION BALANCE
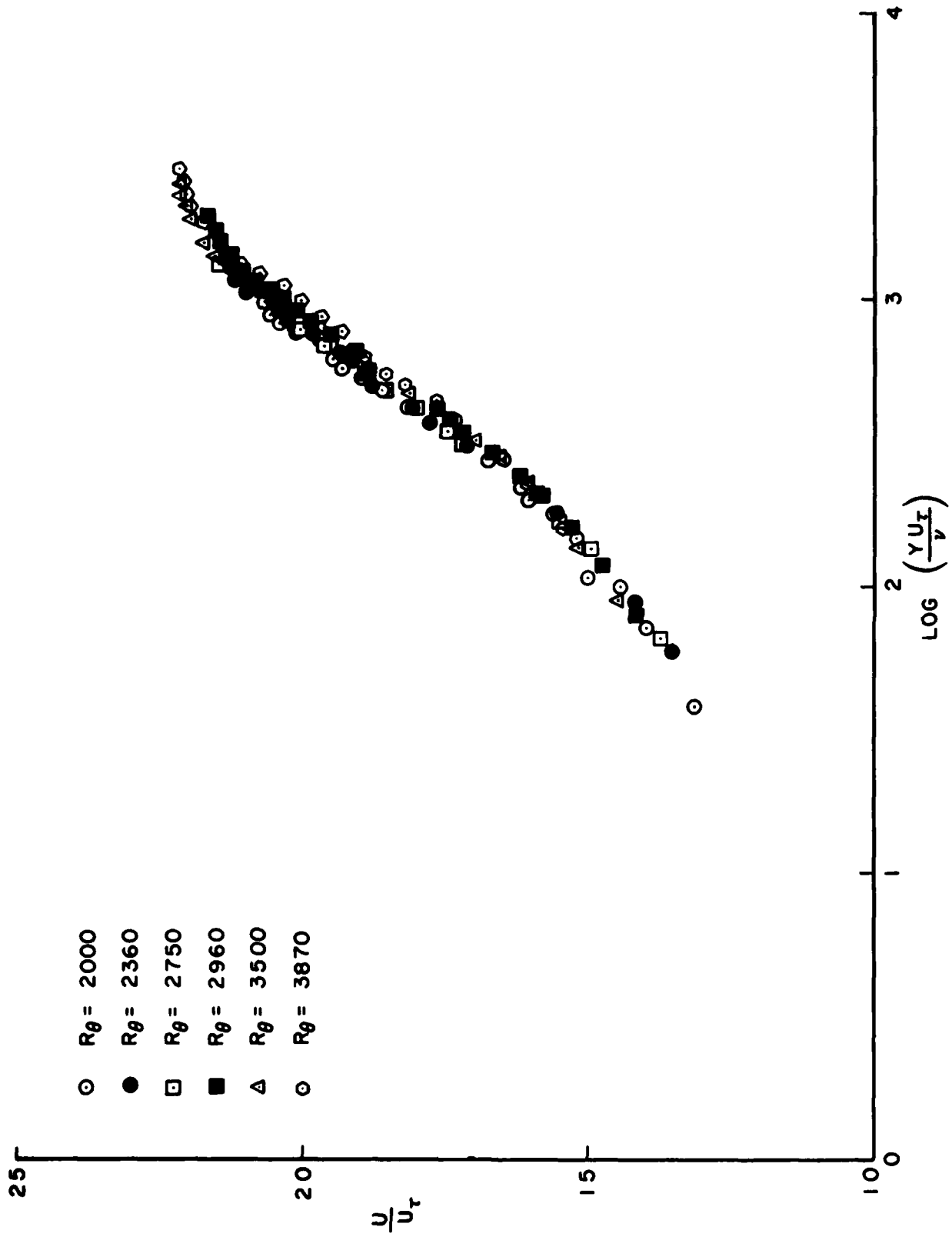
FIG. 4: A CLAUSER PLOT OF THE VELOCITY PROFILES
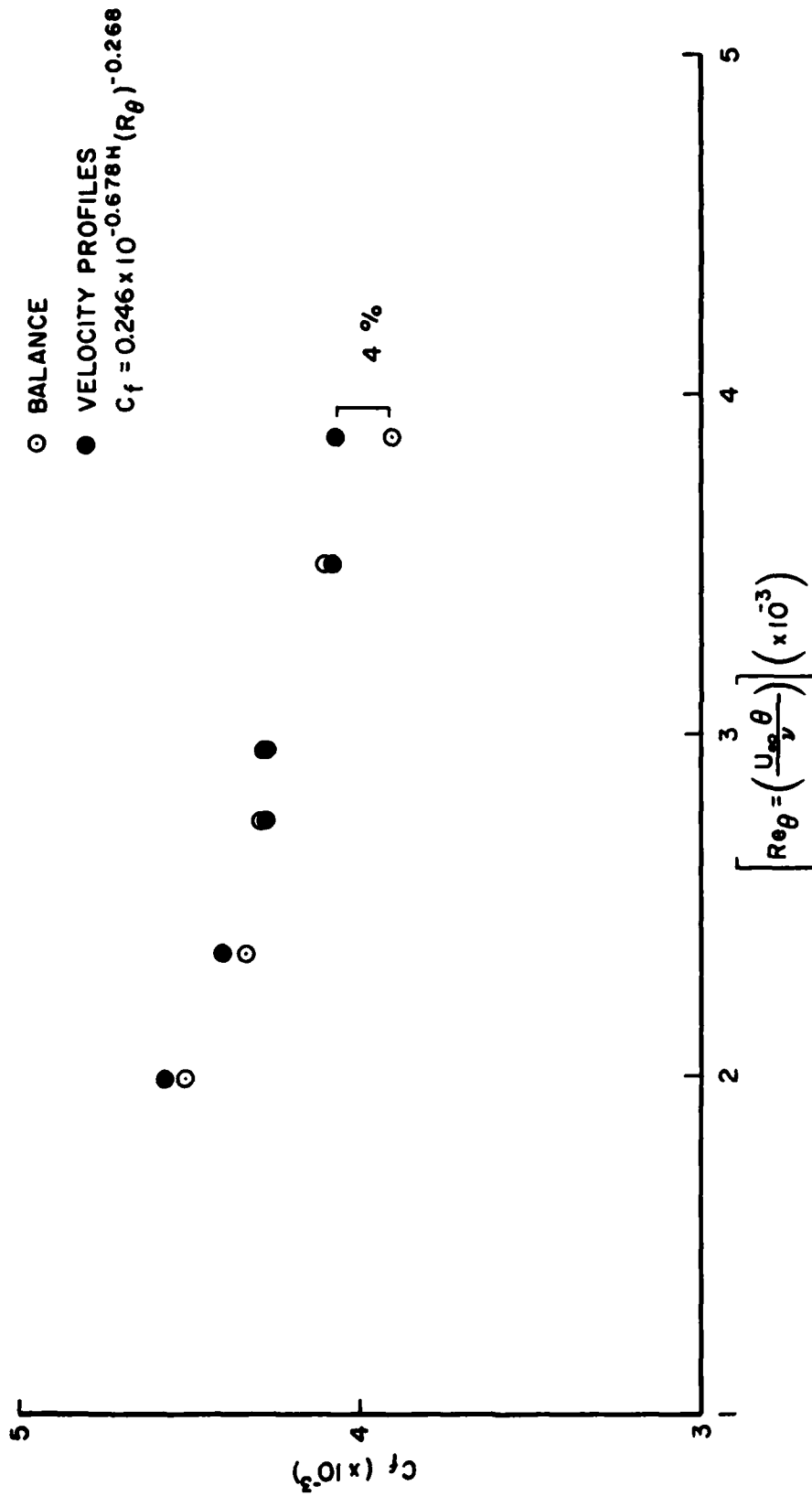
FIG. 5: SKIN FRICTION PLOTTED AGAINST REYNOLDS NUMBER BASED
ON THE MOMENTUM THICKNESS C_f (x) v Re(θ)
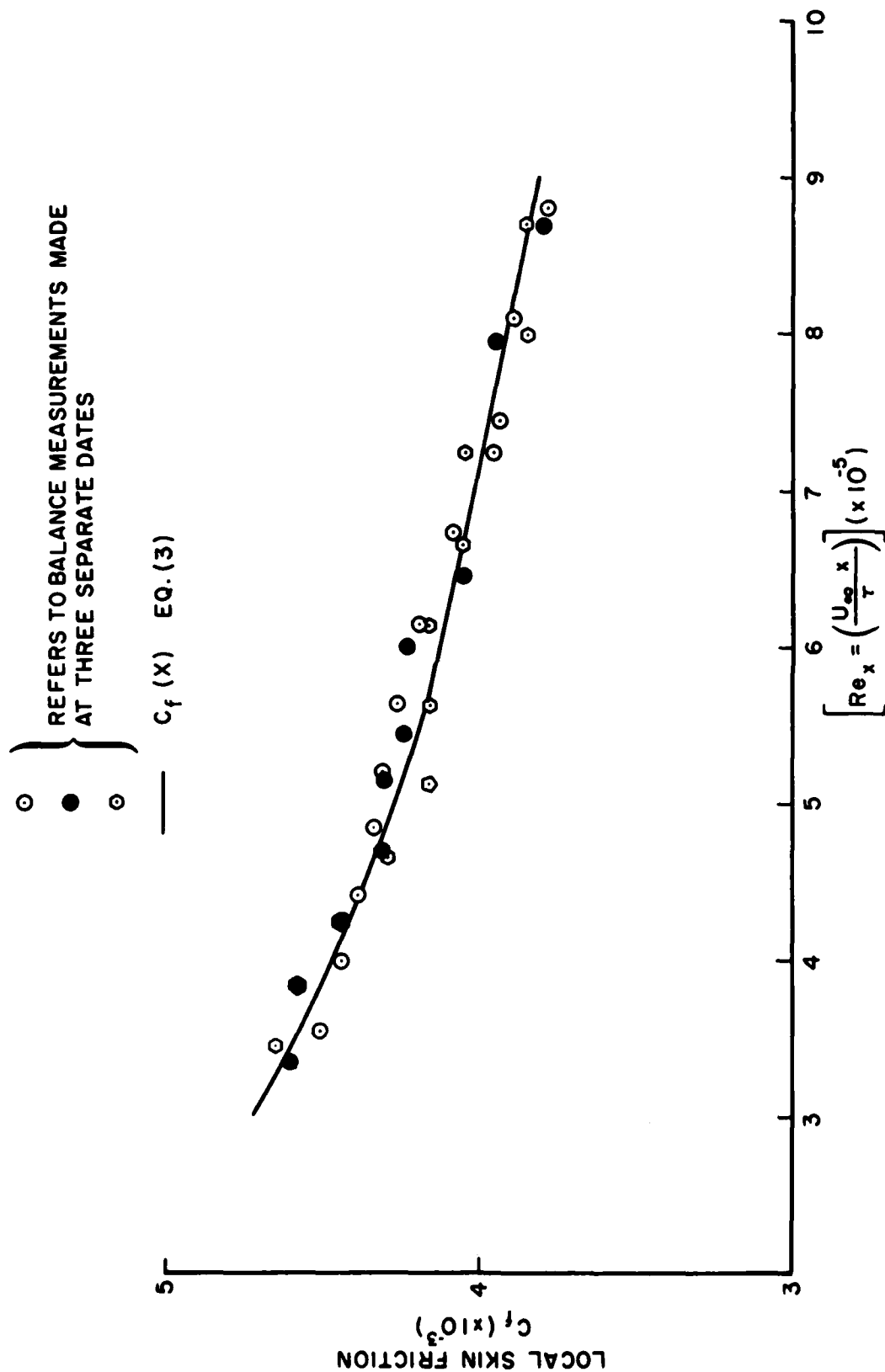
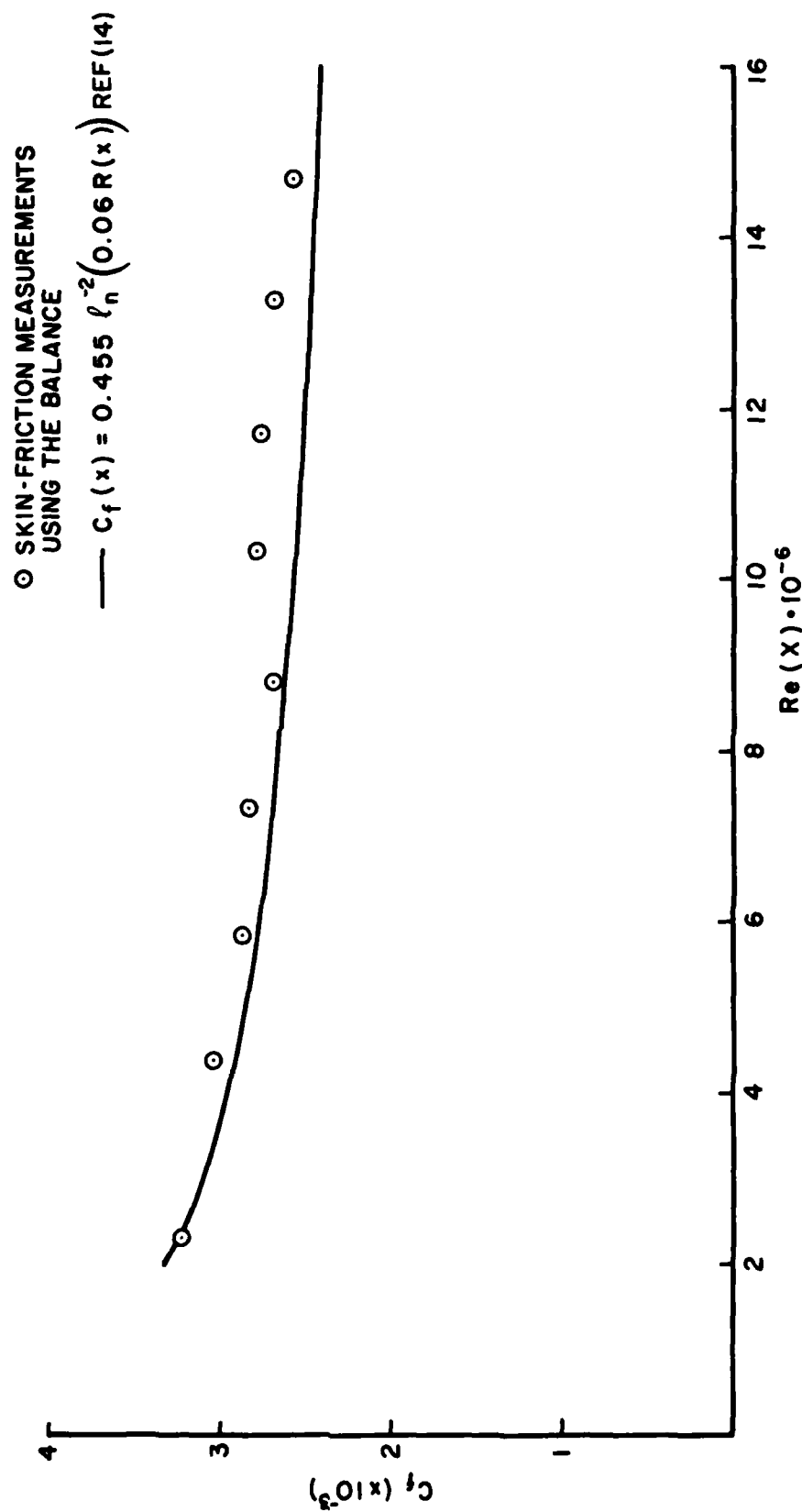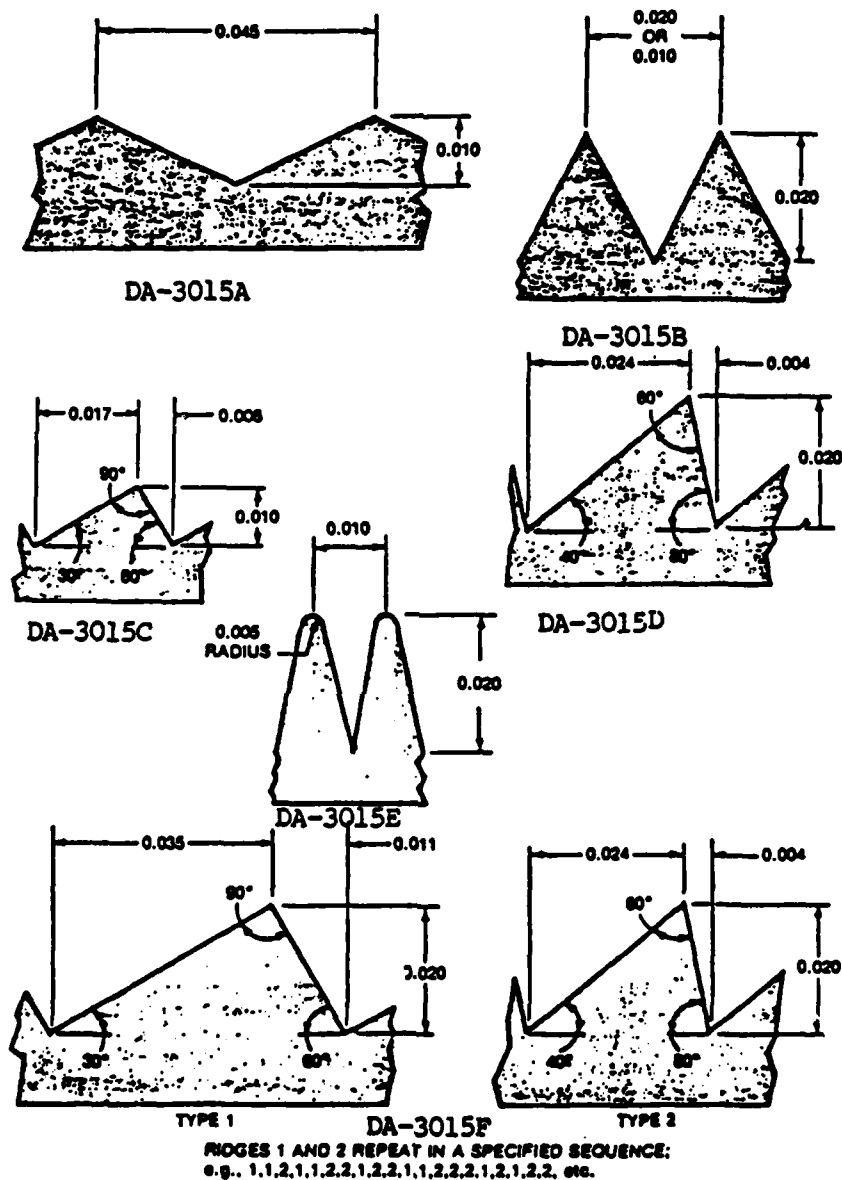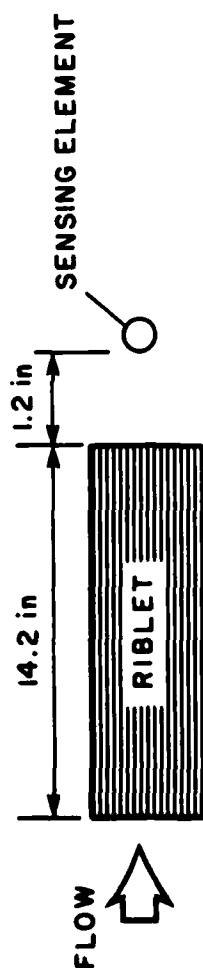FIG. 6: SKIN FRICTION PLOTTED AGAINST THE LOCAL REYNOLDS NUMBER; $C_f(x)$ v $Re(x)$

⊙ SKIN-FRICTION MEASUREMENTS USING THE BALANCE

$$C_f(x) = 0.455 \, \ell_n^{-2}\left(0.06\,R(x)\right) \text{ REF (14)}$$

FIG. 7: THEORETICAL AND EXPERIMENTAL COMPARISON OF THE SKIN FRICTION VERSUS THE LOCAL REYNOLDS NUMBER IN THE PILOT FACILITY

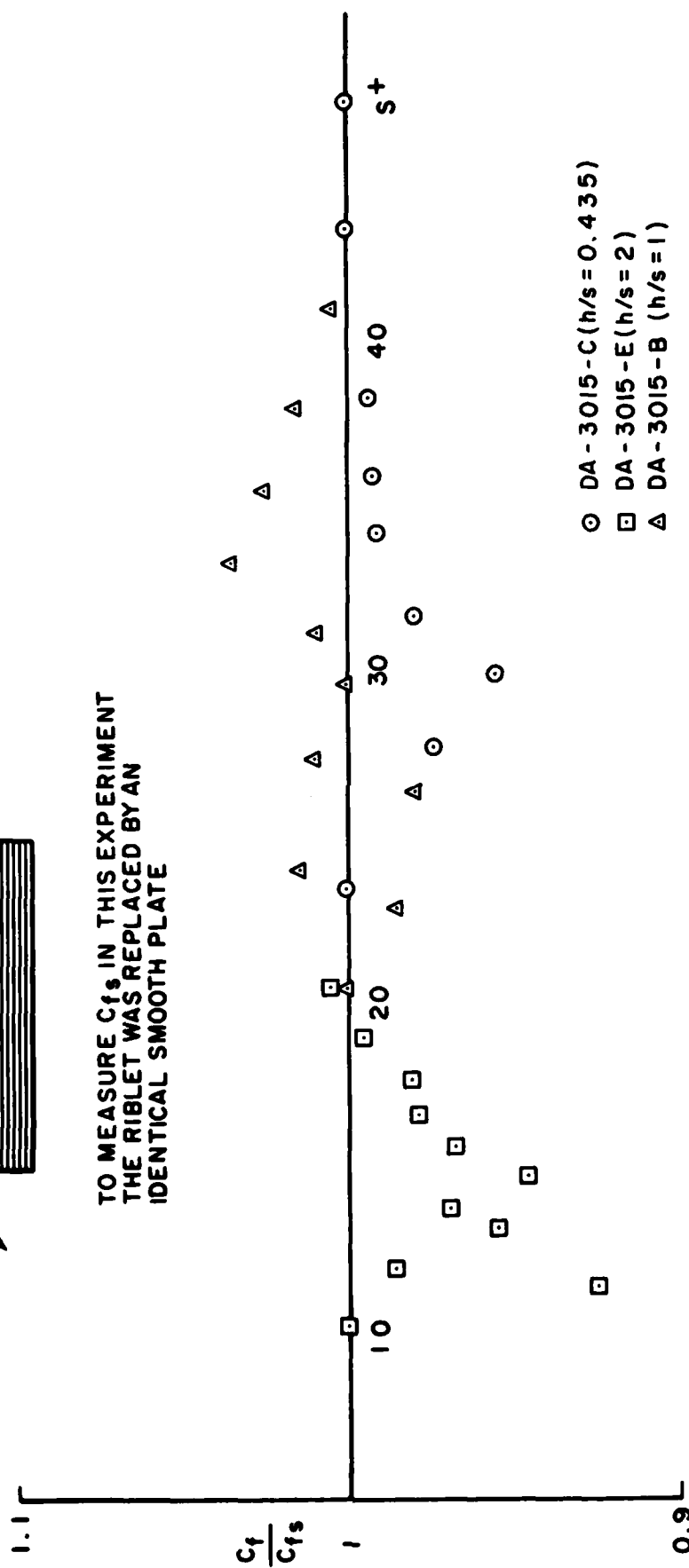FIG. 8: THE EFFECTIVE GROOVED RIBLET GEOMETRIES IN LITERATURE

- 29 -

FIG. 9: NORMALIZED SKIN FRICTION MEASURED DOWNSTREAM OF THE RIBLET, PLOTTED AGAINST THE SCALING PARAMETER s^+
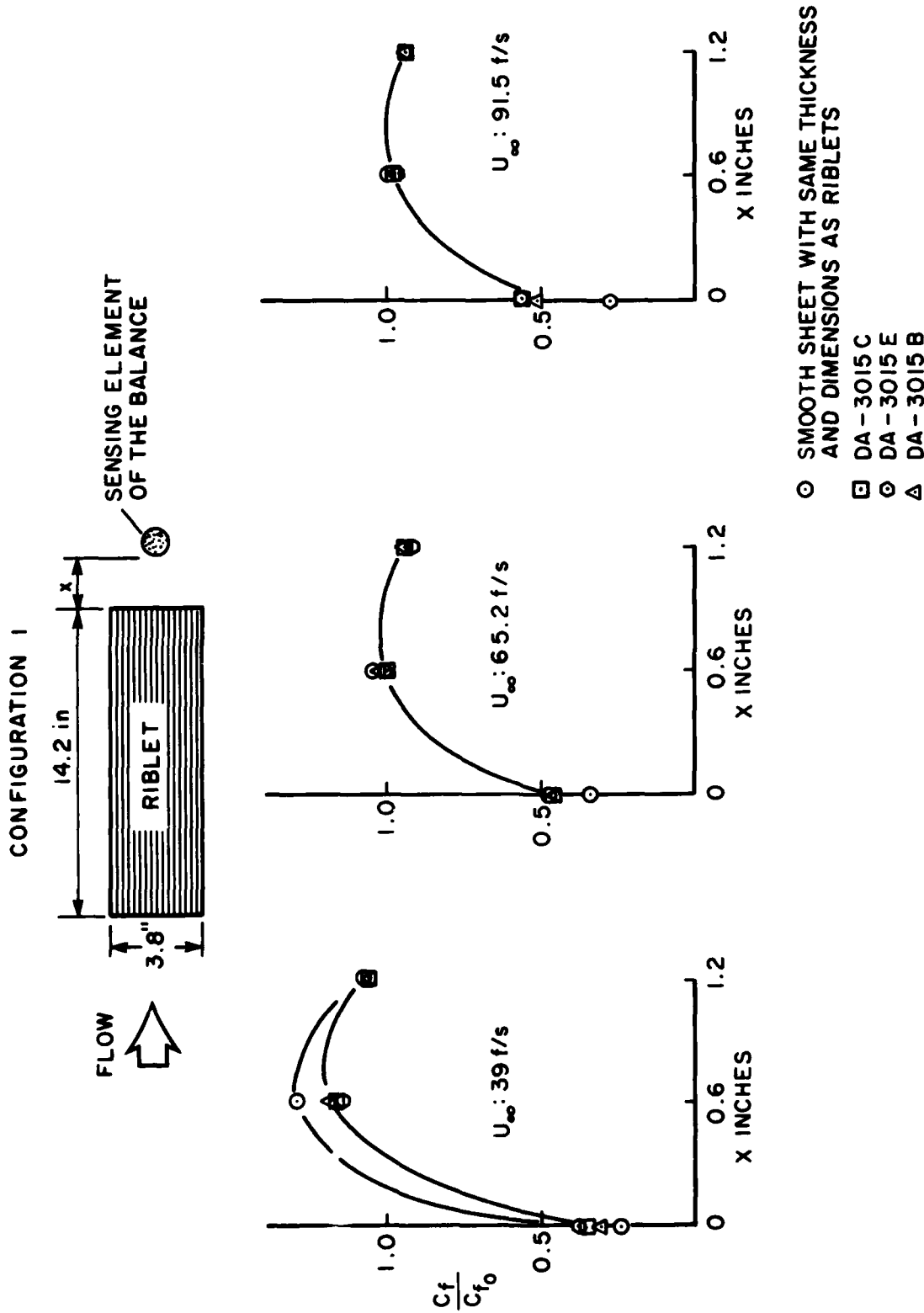
FIG. 10: SKIN FRICTION MEASUREMENTS DOWNSTREAM OF RIBLETS DA-3015B, DA-3015C, DA-3015E AND A CORRESPONDING SMOOTH PLATE AT FLOW VELOCITIES OF 39.0, 65.2 AND 91.5 f/s
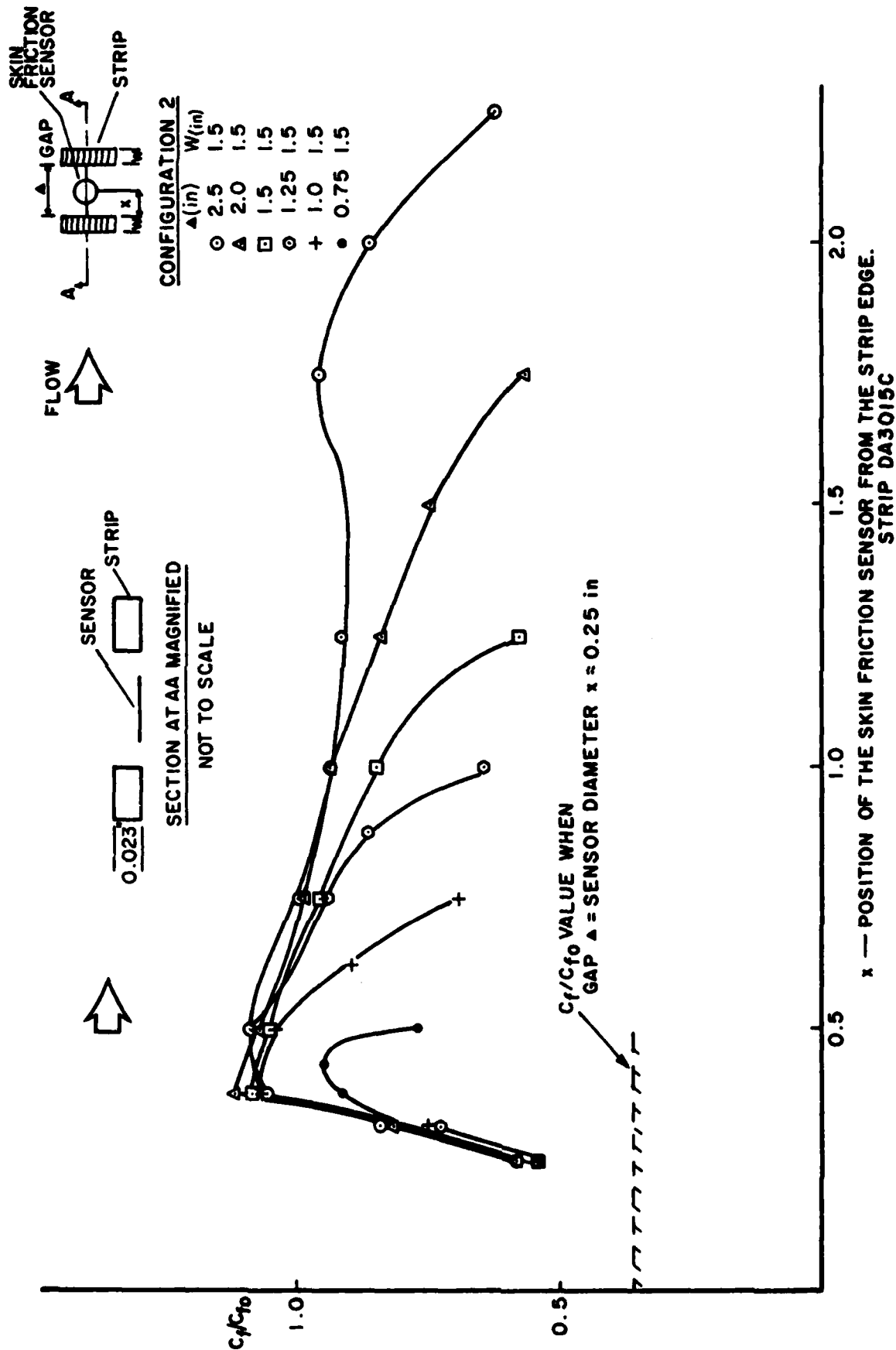
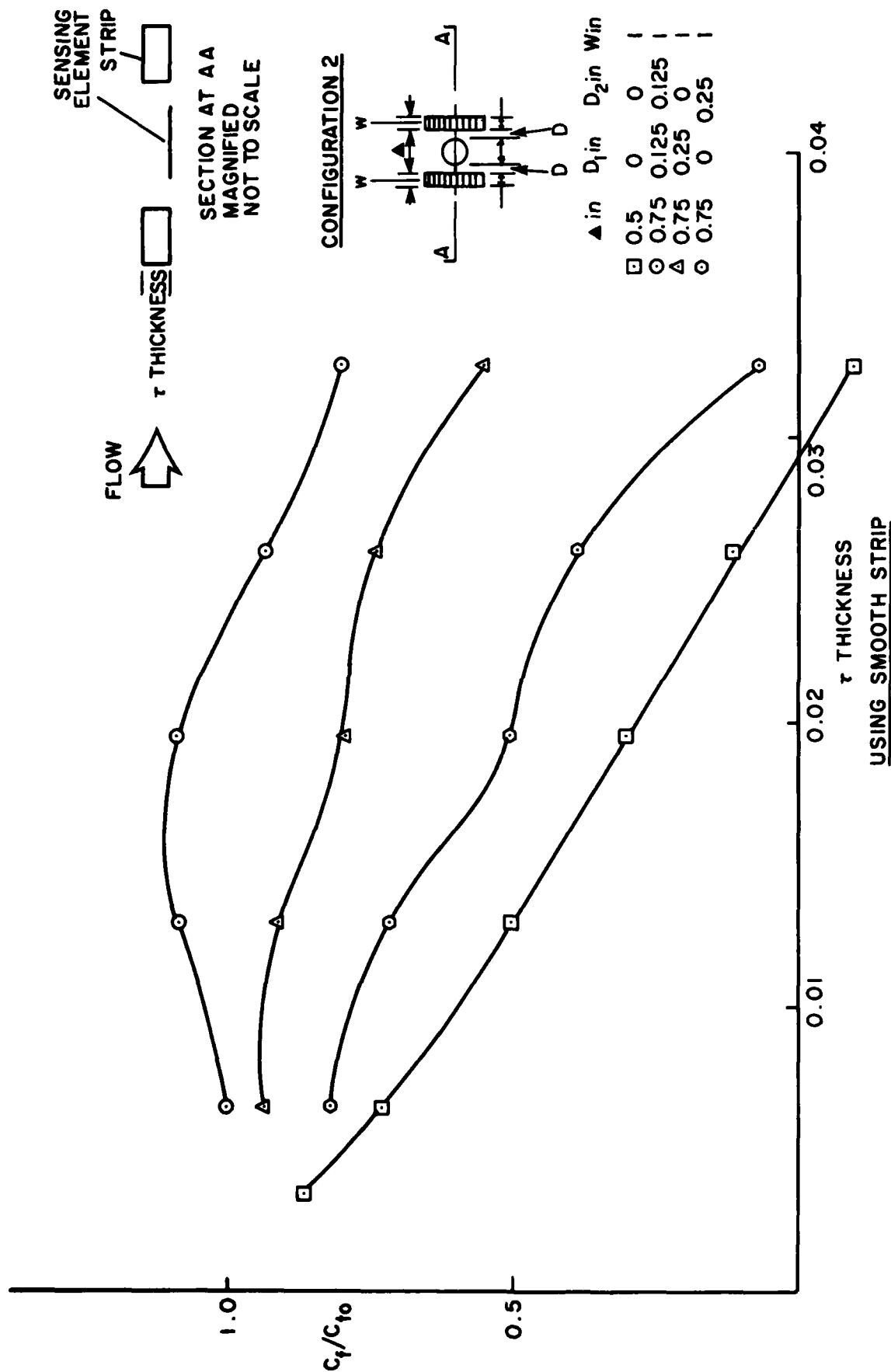FIG. 11: PARAMETRIC STUDY OF STRIP GAP UNDER CONFIGURATION 2

FIG 12: SKIN FRICTION MEASUREMENTS FOR VARIOUS STRIP-THICKNESSES; EFFECT OF GAP AND SENSOR LOCATION IS ALSO SHOWN — CONFIGURATION 2
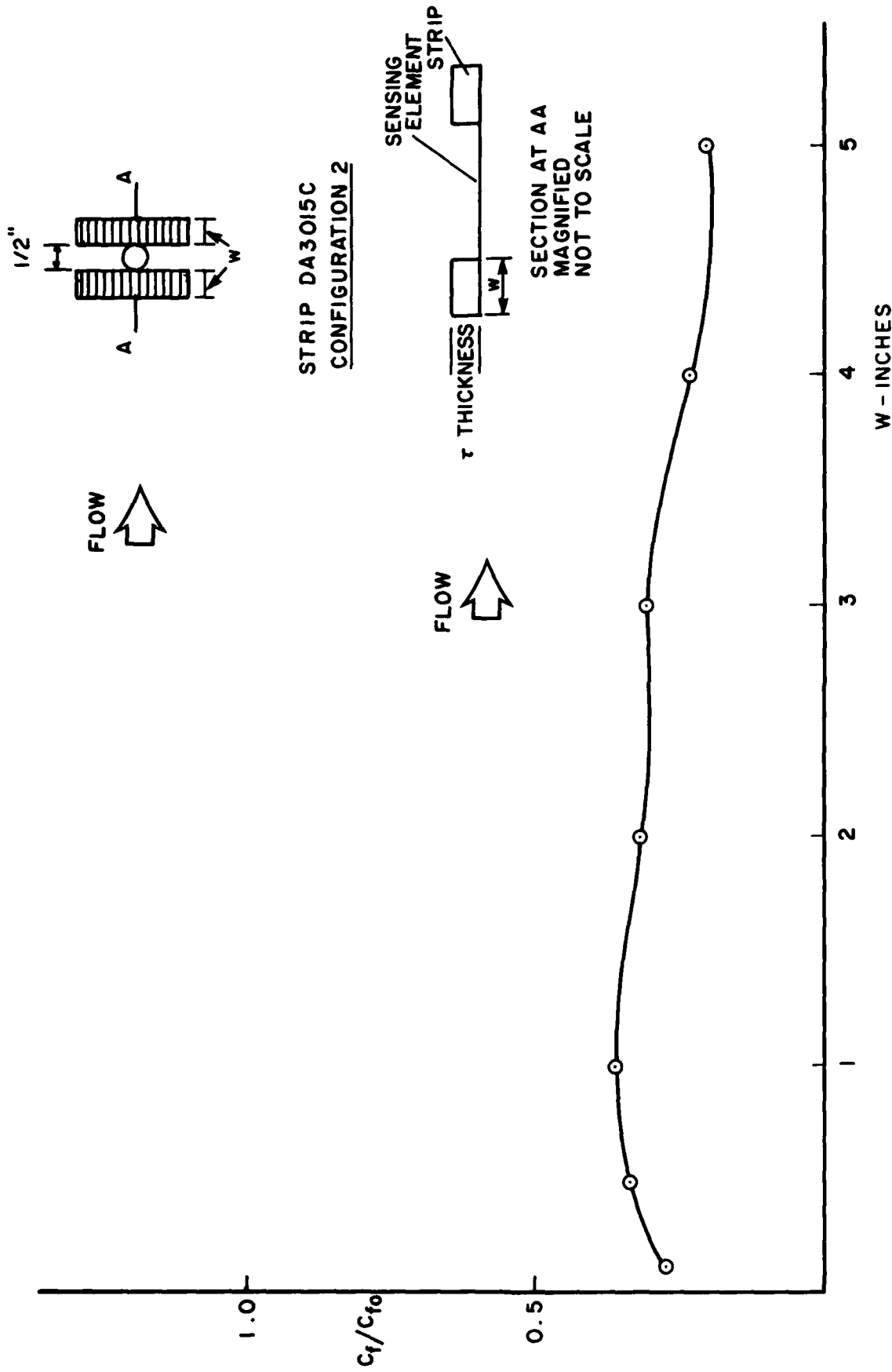
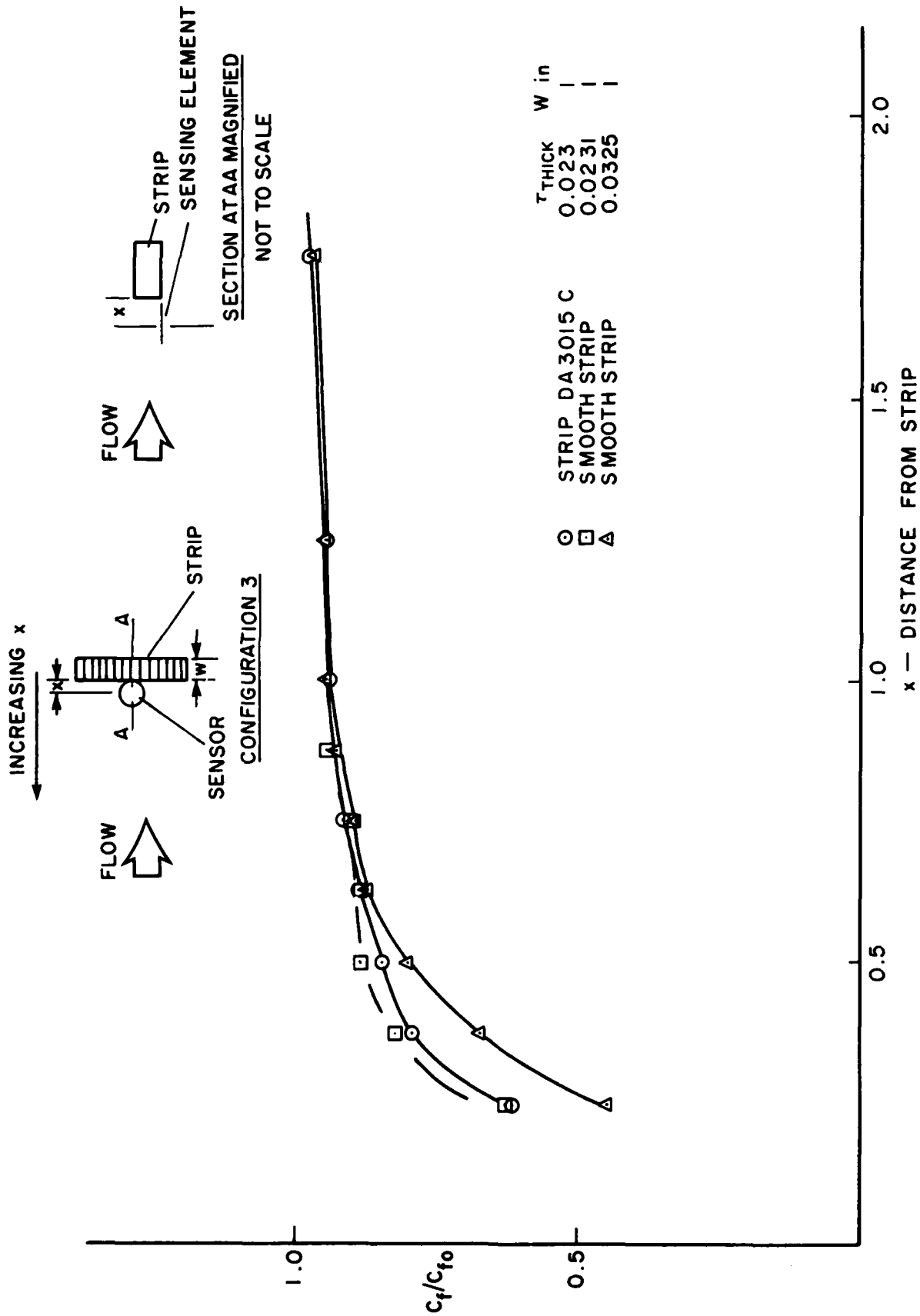FIG. 13: EFFECT OF STRIP WIDTH UNDER CONFIGURATION 2

FIG. 14: SKIN FRICTION MEASUREMENTS FOR THREE STRIP TYPES PLACED AT
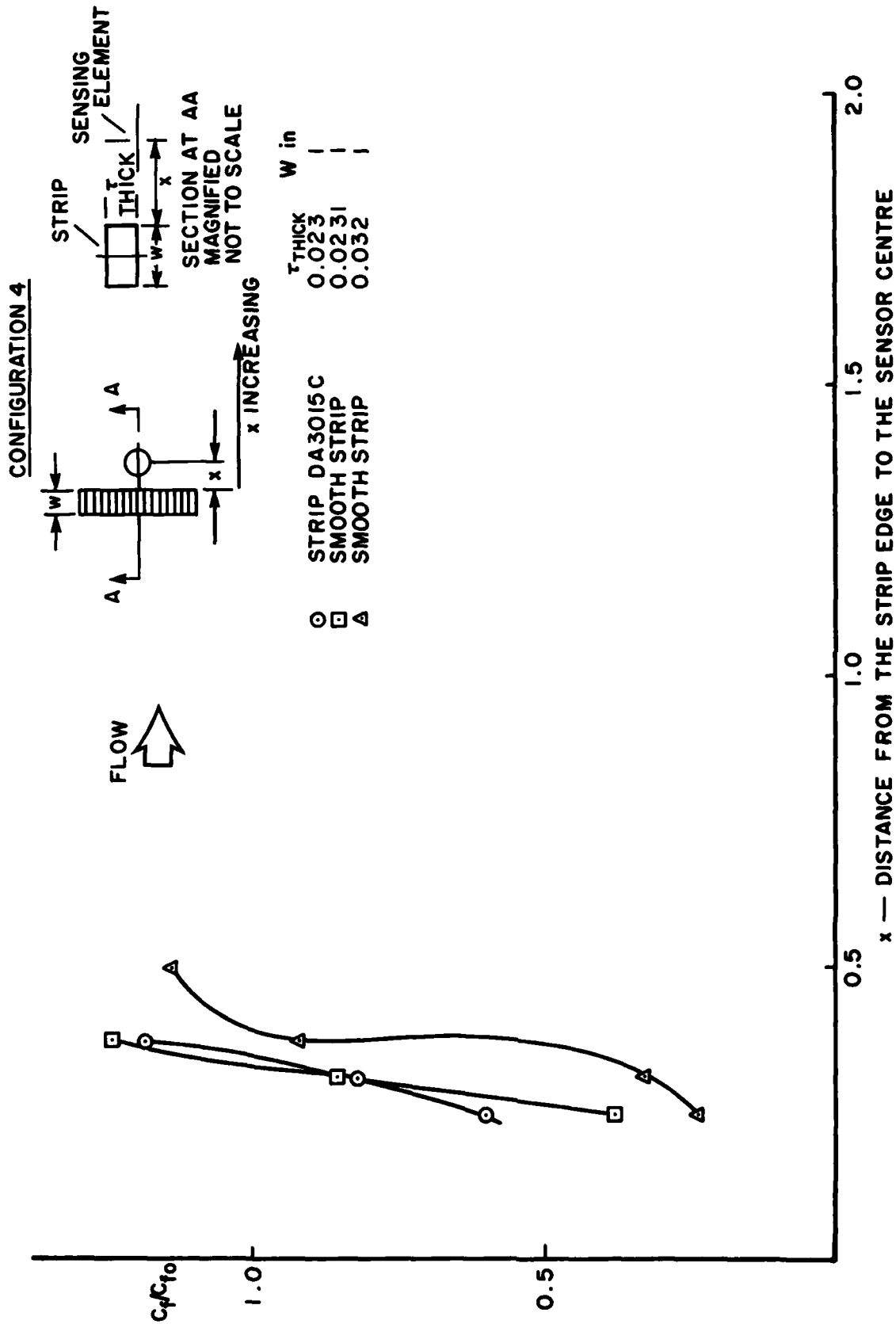DISTANCE x FROM SENSOR — SEE CONFIGURATION 3

FIG. 15: SKIN FRICTION MEASUREMENTS UNDER CONFIGURATION 4

REPORT DOCUMENTATION PAGE / PAGE DE DOCUMENTATION DE RAPPORT

REPORT/RAPPORT	REPORT/RAPPORT
NAE-AN-39 1a	NRC No. 26163 1b

| REPORT SECURITY CLASSIFICATION
 CLASSIFICATION DE SÉCURITÉ DE RAPPORT

 2   Unclassified | DISTRIBUTION (LIMITATIONS)

 3   Unlimited |

TITLE/SUBTITLE/TITRE/SOUS-TITRE

4   An Experimental Investigation of Skin Friction on Smooth Surfaces Supporting Air Bearing Channels

AUTHOR(S)/AUTEUR(S)

5   M. Khalid

SERIES/SÉRIE

6   Aeronautical Note

CORPORATE AUTHOR/PERFORMING AGENCY/AUTEUR D'ENTREPRISE/AGENCE D'EXÉCUTION

National Research Council Canada

7   National Aeronautical Establishment   High Speed Aerodynamics Laboratory

SPONSORING AGENCY/AGENCE DE SUBVENTION

8

DATE 86-07 9	FILE/DOSSIER 10	LAB. ORDER COMMANDE DU LAB. 11	PAGES 40 12a	FIGS/DIAGRAMMES 15 12b

NOTES

13

DESCRIPTORS (KEY WORDS)/MOTS-CLÉS

1. Skin friction drag reduction   4. Skin friction balance
2. Air bearing channels   5. Laminar sublayer
14   3. Riblets

SUMMARY/SOMMAIRE

     A new method, to obtain skin friction reduction by installing air-bearing channels on a smooth surface in uniform flow was investigated. The measurements were made by a servo-controlled skin friction balance. The parametric studies of the channel having step dimensions less than the laminar sublayer thicknesses and placed in flows of free stream velocity up to 90 ft/s have shown that an average skin friction reduction of 25% in the air-bearing cavity is well within reach. It was also confirmed that riblet-type surface grooves can produce up to 10% skin friction drag reduction.

15

END

10-86

DTIC